Modelling of ethanol decomposition on Pt(111): a comparison with experiment and density functional theory

2005 J. Phys.: Condens. Matter 17 6139

(http://iopscience.iop.org/0953-8984/17/39/003)

INSTITUTE OF PHYSICS PUBLISHING JOURNAL OF PHYSICS: CONDENSED MATTER

J. Phys.: Condens. Matter **17** (2005) 6139–6148 doi:10.1088/0953-8984/17/39/003

Modelling of ethanol decomposition on Pt(111): a comparison with experiment and density functional theory

E Vesselli[1,2,3,4], **G Coslovich**[1], **G Comelli**[1,2,3] **and R Rosei**[1,2,3]

[1] Physics Department, Università degli Studi di Trieste, via A. Valerio 2, 34127-Trieste, Italy
[2] Center of Excellence for Nanostructured Materials, Università degli Studi di Trieste, via A. Valerio 2, 34127-Trieste, Italy
[3] Laboratorio Nazionale TASC-INFM, Area Science Park, S.S. 14 km 163.5, 34012-Basovizza (Trieste), Italy

E-mail: vesselli@tasc.infm.it

Received 27 July 2005
Published 16 September 2005
Online at stacks.iop.org/JPhysCM/17/6139

Abstract

Ethanol decomposition on the clean Pt(111) surface has been studied in the zero-coverage limit within the framework of the unity bond index-quadratic exponent potential (UBI-QEP) model. Previous work, both experimental and theoretical, was already available in the literature on this reaction. The system has therefore been used as a benchmark for evaluating the accuracy of the simple phenomenological UBI-QEP model. The latter allows the estimation of key reaction parameters such as adsorption energies and reaction barriers. The stability of possible dissociation intermediates has been investigated and the most probable decomposition pathway has been simulated by integration of the related rate equations. We find that the model provides good estimates for adsorption energies of mono-coordinated molecules with long bond distances and gives realistic values for dehydrogenation barriers. Poor agreement with density functional theory (DFT) is found in the estimates of C–C and C–O bond cleavage barriers, even though the results obtained are in line with the experiments. It is found that transition and final state energies obtained from the model satisfy the linear Brønsted–Evans–Polanyi relation. Temperature programmed desorption spectra and surface coverage of the adspecies as a function of the temperature have been simulated in order to provide a direct comparison with previous experimental data. A possible pathway for ethanol decomposition on Pt(111) is finally proposed on the basis of the present calculations, conciliating previous DFT and experimental results.

[4] Author to whom any correspondence should be addressed.

1. Introduction

Pt and Rh based catalysts are currently being developed for the ethanol reforming reaction, which is a possible candidate for effecting renewable hydrogen production [1, 2]. Investigation of the mechanisms for EtOH (CH_3CH_2OH) decomposition on model transition metal surfaces can therefore provide useful insights, yielding valuable kinetic and chemical information for the comprehension of the reaction steps.

Decomposition of EtOH on Pt(111) has already been studied [3–5] and additional information on the dehydrogenation mechanism has recently been obtained with the aid of spectroscopic surface science techniques [6]. For comparison, we will here focus on the results which have been recently obtained within the density functional theory (DFT) framework by Alcalá and co-workers [3], as well as on spectroscopic UHV experimental data obtained by Lee *et al* [6]. The latter have been obtained by temperature programmed desorption (TPD) and high resolution synchrotron radiation x-ray photoelectron spectroscopy (XPS) measurements.

DFT calculations identify ethanol, 1-hydroxyethyl (CH_3CHOH), 1-hydroxyethylidene (CH_3COH), acetyl (CH_3CO), ketene (CH_2CO), ketenyl (CHCO) and CCO as the most stable intermediates for each dehydrogenation step from six to zero H atoms containing molecules. Moreover, it is found by *ab initio* methods that 1-hydroxyethylidene (CH_3COH) has the lowest transition state energy for C–O cleavage (with a decomposition barrier of 1.0 eV), while the ketenyl intermediate (CHCO) shows the lowest decarbonylation barrier (0.95 eV). These results, combined with transition state theory, predict that the C–C cleavage reaction is faster than C–O dissociation on Pt(111) at temperatures above 550 K [3].

Under UHV conditions, it is experimentally demonstrated that ethanol adsorbs molecularly at 100 K on Pt(111) [5, 6]. The decomposition reaction at higher temperature proceeds by progressive dehydrogenation to a metastable intermediate (which is tentatively identified with acetyl—CH_3CO). Subsequently, the latter molecule undergoes dehydrogenation and decarbonylation to form CO and CH or CH_3 groups via C–C bond cleavage. It is assumed that CH_x groups can both hydrogenate to methane (which is indeed detected in the TPD experiments [6]) and decompose into adsorbed hydrogen and carbon atoms. Since DFT calculations propose ketenyl (CHCO) as the intermediate with the lowest C–C cleavage barrier, it is proposed that acetyl dehydrogenates to ketenyl (unstable), which decomposes into CO and CH. CH groups finally rehydrogenate to methane.

In the present work, we discuss the role that a simple phenomenological model such as the unity bond index-quadratic exponent potential (UBI-QEP) [7, 8] can play in the evaluation of reaction parameters. Adsorption energies, dehydrogenation barriers and activation energies for C–C, C–O, C–H and O–H bond cleavage have been evaluated using this model for a number of possible reaction intermediates of the ethanol dissociation reaction on Pt(111). This allowed us to obtain a benchmark for such a simple tool, which provides direct estimates for key reaction parameters. The input for the calculations was obtained from already available experimental and *ab initio* data. We discuss the results by comparing the calculated adsorption energies and reaction barriers with previous theoretical and experimental data. Finally, we simulate ethanol decomposition and propose a tentative picture of the reaction pathway, which is in agreement with previous work.

2. Calculation details

Adsorption energies and reaction barriers were calculated within the framework of the UBI-QEP model [7, 8]. As the only inputs of the calculations, we used values of adsorption (atomic and molecular), bond and dissociation energies taken from the literature [3, 9–15].

Best adsorption geometries were also obtained from previous works, when available. When not, adsorption energy values for differently coordinated sites were obtained within the UBI-QEP model. Unknown molecular adsorption energies were instead calculated from the atomic binding energies.

The model allows the calculation of several physical quantities relevant for chemisorption and catalytic systems. Hereafter, we report only the equations used in the present study.

The atomic heat of adsorption for an atom A bonded in n-fold geometry on a single-crystal surface, $Q_{A,n}$, can be calculated from the adsorption energy in the on-top site, $Q_{A,0}$ (equation (1)):

$$Q_{A,n} = Q_{A,0}\left(2 - \frac{1}{n}\right). \tag{1}$$

For a diatomic molecule AB, there are three types of molecule–surface interaction considered by the model: weak, medium and strong binding. Weak binding occurs for closed-shell molecules (e.g. CO, N_2, H_2O, NH_3, CH_3CO) and molecules with strongly delocalized unpaired electrons (e.g. O_2, NO); in this case, if the molecule adsorbs via the A atom in an n-fold site, the adsorption energy is given by (equation (2))

$$Q_{AB,n} = \frac{Q_{A,0}^2}{\frac{Q_{A,0}}{n} + D_{AB}} \tag{2}$$

where D_{AB} is the dissociation energy, which in this case equals the bond energy. Strong binding occurs for molecular radicals with localized electrons such as OH, CH and CH_3O. In this case, the adsorption energy is given by (equation (3))

$$Q_{AB,n} = \frac{Q_{A,n}^2}{Q_{A,n} + D_{AB}}. \tag{3}$$

In the medium binding condition, valid for monovalent radicals like the methyl group, the binding energy is calculated as the average of the previous two.

Polyatomic molecules are treated as an extension of the diatomic case: if A is the atom which binds to the surface, B is defined as the rest of the molecule; for mono-coordination the equations remain the same as for the diatomic case.

For asymmetric di-coordination of a chelated molecule A–X–B which binds to the surface with both A and B atoms to on-top sites, the total binding energy is given by (equation (4))

$$Q_{AXB} = Q_{0AX} + Q_{0BX} - \frac{Q_{0AX}Q_{0BX}}{Q_{0AX} + Q_{0BX}}. \tag{4}$$

For the dissociation of an AB molecule to A and B fragments, the enthalpy change ΔH and the reaction barrier ΔE_{AB} are evaluated as (equation (5))

$$\begin{aligned} \Delta E_{AB} &= \frac{1}{2}\left(\Delta H + \frac{Q_A Q_B}{Q_A + Q_B}\right) \\ \Delta H &= D_{AB} + Q_{AB} - Q_A - Q_B. \end{aligned} \tag{5}$$

3. Results and discussion

3.1. Adsorption energies of possible reaction intermediates

Heats of adsorption of the possible reaction intermediates for ethanol decomposition on Pt(111) have been evaluated with the UBI-QEP model for direct comparison to the values computed with DFT methods in [3]. The results are summarized in figure 1. It can be observed that the general trend is qualitatively reproduced on the eV scale with few exceptions.

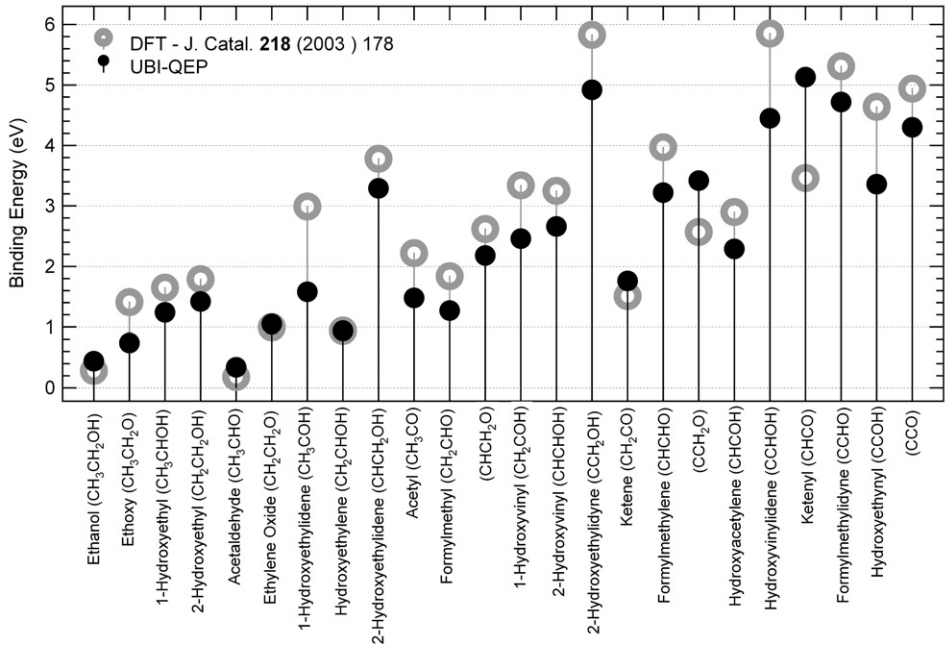

Figure 1. Plot of the molecular heats of adsorption of the possible reaction intermediates for the ethanol decomposition reaction on Pt(111) as obtained from the UBI-QEP model and (for comparison) from DFT computations in [3].

Best results are obtained when the UBI-QEP model is applied only once. As an example, the adsorption energies for acetaldehyde (CH_3CHO) and hydroxyethylene (CH_2CHOH) can be compared. In the former case, the molecule is doubly coordinated and binds to the metal surface via its oxygen and carbon atoms in an on-top configuration. The atomic binding energies in the on-top sites are evaluated from the hollow site values and in a second step the molecular heat of adsorption is calculated. The model is therefore applied twice. A UBI-QEP value for the binding energy of 0.34 eV is obtained, to be compared to the DFT value of 0.18 eV [3], leading to a relative error of about 50%. In the case of hydroxyethylene, in contrast, which binds to the metal via the carbon atoms, atomic binding energies in the right adsorption sites are already available in the literature [16, 17]. Indeed, the value of 0.94 eV is perfectly reproduced [3]. In general, it has been observed that the input data are of core importance. When considering DFT calculations, for example, it is well known that relative energy differences can be evaluated with great accuracy. In contrast, absolute values can differ substantially from one framework to another. Therefore, when more than one source is used for the input parameters of a UBI-QEP calculation, care has to be taken because errors are then propagated and amplified through the whole calculation. As an example, the CO heat of adsorption is available both from the experiment and from DFT. Values of 1.43 [16] and up to 2.12 eV [18] have been reported, respectively. It is clear that initial errors of 50% can dramatically affect the UBI-QEP results. Within the present work, DFT values have been considered as a reference for the model, even though it is known that *ab initio* frameworks can fail in the treatment of some interactions, yielding underestimation or overestimation of the associated energies. Discrepancies between results from the two frameworks are therefore not necessarily indicating a failure of the simple model, even though DFT methods are with no doubt the most reliable *ab initio* resources at present.

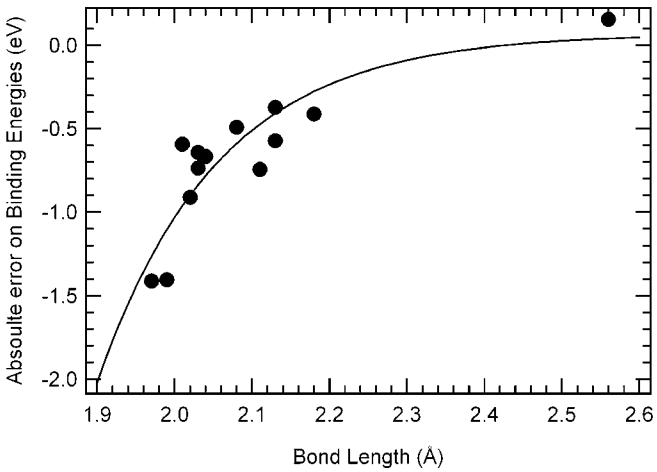

Figure 2. Error in the calculated heats of adsorption as obtained from the UBI-QEP model with respect to values from DFT in [3]. Data for mono-coordinated molecules have been plotted as a function of the bond length [3] to the metal atoms. Fitting with an exponential function has been plotted in the graph to guide the eye.

For the model calculations, a clear correlation between the error on the heats of adsorption and the bond lengths has been observed. In figure 2, the differences between UBI-QEP and DFT adsorption energies for mono-coordinated intermediates have been plotted as a function of the bond distance calculated by DFT methods in [3]. Data have been fitted with an exponential function to guide the eye. It is evident that the shorter the equilibrium distance, the bigger the error (for the defect) due to the model. This can be tentatively explained by referring to the bond index definition which is at the basis of the whole UBI-QEP model. Bond indices are defined as polynomial functions of exponentials, under the assumption that atomic functions' radial parts show this profile. This is indeed true for large distances from the core, while, at short bond lengths, overlap of charge densities with profiles which deviate from an exponential shape occurs [19]. It can be concluded that the UBI-QEP model tends to underestimate binding energies for bond lengths shorter than 2.2 Å.

3.2. Ethanol decomposition

3.2.1. Reaction barriers. *Ab initio* C–C and C–O dissociation energies for the most stable reaction intermediates were already available in [3]: the most favourable intermediate for C–O bond scission was found to be 1-hydroxyethylidene (CH_3COH). The UBI-QEP model identifies, in addition to CH_3COH, a second candidate, hydroxyethylene (CH_2CHOH), with the same C–O dissociation barrier. For the decarbonylation reaction, DFT calculations show that the ketenyl intermediate (CHCO) has the lowest dissociation energy. This is confirmed by the UBI-QEP model, provided we exclude the C–C bond scission in acetaldehyde, which, in contrast to DFT results, is found to have the lowest dissociation barrier. It has to be noted that reference DFT values for the barriers in [3] appear to be too high. As an example, C–C bond cleavage activation energies for ketenyl and ketene are found to be 0.95 and 1.34 eV, respectively. This implies that, assuming a standard pre-exponential factor of 10^{13} s^{-1}, bond scission occurs at temperatures higher than 440 K, in contrast with the experiment [6], where CH_x species and CO are observed already below 200 K. In contrast, with the UBI-QEP model,

decomposition barriers of 0.26 and 0.22 eV are obtained for the two species respectively, which are compatible with the experimental dissociation temperatures.

Dehydrogenation barriers for the possible intermediates considered have also been calculated by means of the UBI-QEP model. These values were not computed in the DFT work [3], even though the competition between dehydrogenation and C–C/C–O scissions actually determines the real reaction path. A possible complete dissociation path is instead proposed in [6] on the basis of spectroscopic data and will be discussed later. The reaction path reported in equation (6), was obtained by simple application of the model, considering only subsequent dehydrogenation steps:

$$\begin{aligned} CH_3CH_2OH \xrightarrow{0.52\ eV} CH_3CHOH \xrightarrow{\text{not stable}} CH_3CHO \xrightarrow{0.13\ eV} CH_3CO \xrightarrow{0.29\ eV} \\ CH_2CO \xrightarrow{0.70\ eV} CHCO \xrightarrow{0.50\ eV} CCO. \end{aligned} \tag{6}$$

As a second step, we simulated the whole EtOH decomposition reaction by including also the C–C scission. Decarbonylation of the ketenyl (CHCO) intermediate as well as that of acetyl (CH_3CO) were included in the reaction on the basis of the experimental results. Indeed in [6], CH_3CO is proposed as a stable intermediate in analogy with acetaldehyde decomposition on the same surface, while the ketenyl is the favourable configuration for C–C cleavage. From the model calculation, similar decarbonylation barriers are obtained for the two species (0.26 and 0.22 eV respectively). The final decomposition path yielded by the model contains therefore two parallel channels (see equation (7)), which are generated by the competition between C–H and C–C bond cleavage in the acetyl intermediate:

$$\begin{aligned} & & CH_2CO \rightarrow CHCO \rightarrow CH + CO \\ CH_3CH_2OH \rightarrow CH_3CHO \rightarrow CH_3CO \rightarrow & & \\ & & CH_3 + CO \rightarrow CH_2 + CO \rightarrow CH + CO. \end{aligned} \tag{7}$$

In the work by Alcalá *et al* [3], it is found that computed final and transition state energies for the exothermic decomposition reactions of the possible ethanol dissociation intermediates satisfy the Brønsted–Evans–Polanyi (BEP) linear relation [20, 21]. Such a relationship was known to hold for CH, CO, NO, N_2 dissociative chemisorption on both flat and stepped single-crystal transition metal surfaces [21]. In [3] it is shown that C–C and C–O cleavage in more complex intermediates also follows this 'universal' relation. For comparison, we have therefore computed using UBI-QEP the final and transition state energies of the intermediates considered in [3]. Energy values are referred to the initial gas phase energies. With reference to the UBI-QEP formalism we have that $E_{TS} = -Q_{AB} + \Delta E$ and $E_{FS} = -Q_A - Q_B + D_{AB}$. DFT data and results from the present work are plotted together in figure 3. In [21], angular coefficients (α) of 0.90 ± 0.04 and 0.87 ± 0.05 are obtained for adsorption of molecules on the close-packed surfaces and at steps, respectively. In [3] it is found that $\alpha = 0.97 \pm 0.03$, while the model calculations yield for α the value of 0.94 ± 0.04. This result is apparently non-trivial, since there is no explicit linear dependence of E_{TS} from E_{FS} in the model formalism.

3.2.2. Simulation of the whole decomposition reaction. Rate equations have been written for reaction (7), including also the rehydrogenation of the methyl groups. Three processes have been considered, depending on the intermediates: first-order desorption (equation (8)), recombinative second-order desorption (equation (9)) and the dissociation (equation (10)):

$$\frac{d\theta_{CO}}{dt} = -\nu_0 \theta_{CO} \exp\left(-\frac{E_{des}}{k_B T}\right) \tag{8}$$

$$\frac{d\theta_H}{dt} = -2\nu_0 \theta_H^2 \exp\left(-\frac{E_{des}}{k_B T}\right) \tag{9}$$

$$\begin{aligned}\frac{d\theta_{AB}}{dt} &= -\nu_0\theta_{AB}\exp\left(-\frac{E_{diss}}{k_B T}\right)\\ \frac{d\theta_{A}}{dt} &= +\nu_0\theta_{AB}\exp\left(-\frac{E_{diss}}{k_B T}\right)\\ \frac{d\theta_{B}}{dt} &= +\nu_0\theta_{AB}\exp\left(-\frac{E_{diss}}{k_B T}\right).\end{aligned} \tag{10}$$

A standard pre-exponential factor ν_0 of 10^{13} s^{-1} has been assumed for all surface reactions, as routinely done when no information about the pre-exponentials is available. A linear temperature ramp of 0.4 K s^{-1} has been used for the integration of the rate equations, in analogy with the XPS experiment in [6]. Ethanol desorption (figure 4) has been simulated assuming an initial surface saturation coverage of 0.44 ML (monolayers), as reported in [6]. Desorption curves for the decomposition products (figure 4) have been calibrated assuming that only 0.15 ML of the initial ethanol pre-coverage undergoes decomposition due to the competition between the desorption and dissociation processes, as indicated in [6]. The position of the corresponding experimental TPD peaks is indicated in the figure by arrows. Ethanol desorption is remarkably well reproduced by the model. An ethanol dehydrogenation barrier of 0.52 eV and a binding energy of 0.44 eV are obtained. In agreement with the experiment, two main desorption states are present for hydrogen: the peak at lower temperature is desorption limited due to the first dehydrogenation steps of the ethanol molecule; the feature at about 400 K is correlated to the CH_x decomposition. Carbon monoxide is instead only desorption limited. The mass 28 peak position depends therefore only on the desorption energy value, which is in the real case influenced by coverage and co-adsorption effects, not considered in the present modelling.

CH_4 desorption was detected in the TPD experiments and was assigned to subsequent rehydrogenation of the CH groups which form upon decomposition of ketenyl [6], while we propose that methane originates from hydrogenation of adsorbed methyl groups. By means of isotopic experiments [17, 22, 23], it has been shown that methyl groups can easily hydrogenate

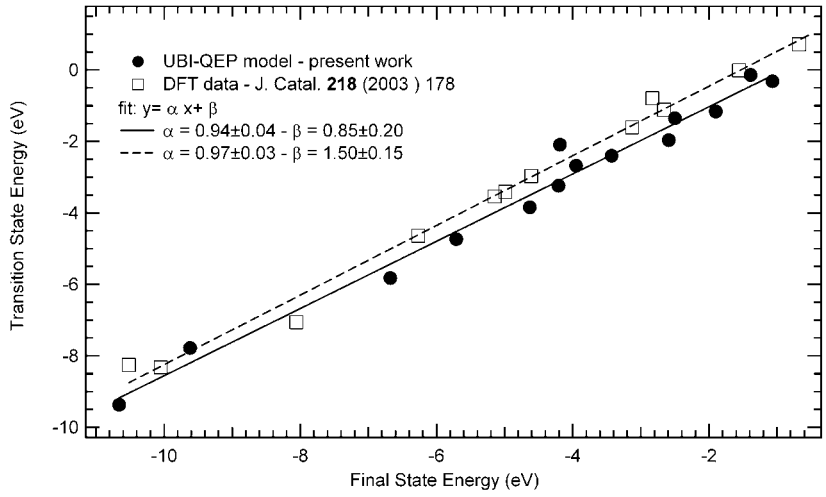

Figure 3. Plot of the transition state energies as a function of the final state energies for the dissociation of relevant intermediates in the ethanol decomposition pathway on Pt(111). Energy values are referred to the initial state in the gas phase. Data from the present work obtained within the framework of the UBI-QEP model are compared to DFT results from [3].

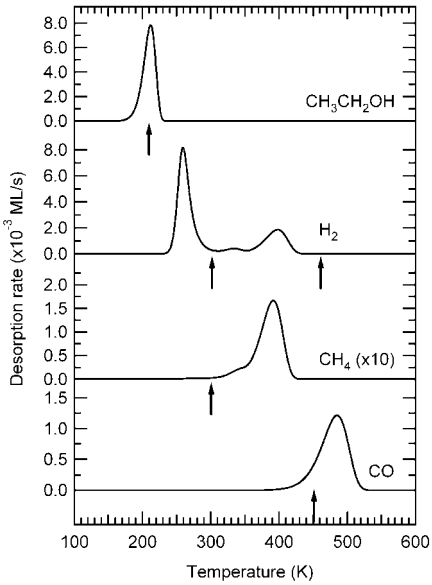

Figure 4. Simulated TPD spectra, obtained on the basis of the results from the UBI-QEP model for ethanol decomposition on Pt(111). The arrows indicate the position of the experimental desorption peaks [6].

to methane on Pt(111). It is also well known that the surface chemistry of CH_3 groups adsorbed on Pt(111) is characterized by a competition between hydrogenation (to CH_4) and dehydrogenation to carbon and hydrogen atoms [17]. Moreover, the hydrogenation probability for adsorbed methylene (CH_2) and methylidyne (CH) groups to methane is significantly smaller than that for CH_3 [22]. CH hydrogenation barriers as high as 0.7 eV have been obtained by means of DFT calculations and the instability of CH_2 has also been shown (the dehydrogenation barrier is about 0.15 eV [24]). On the basis of the present calculation we therefore propose a dual reaction path (see equation (7)). Acetyl (CH_3CO) most probably dissociates via C–C bond cleavage (0.26 eV), rather than dehydrogenating (0.29 eV). Indeed, only about 15% of the decomposing ethanol dissociates through the ketene intermediate (CH_2CO) and subsequently via ketenyl (CHCO) to CH and CO. This picture provides a clear explanation to the CH_4 desorption peak observed experimentally [6]. The authors in [6] propose only tentatively CH_3CO as a stable intermediate, which cannot be unequivocally identified from the C 1s features in the XPS spectra, while they suggest that C–C cleavage occurs in the ketenyl.

In figure 5, computed surface species concentrations are plotted as a function of the linear annealing temperature as in the reference XPS experiment [6]. The temperature range in which each species is found to be stable on the basis of XPS data is indicated by the arrows. Only the contribution from ethanol which undergoes decomposition is reported, while EtOH desorption is considered for the TPD experiment only (figure 4). The CH_3 and CH trends are well reproduced. Carbon monoxide desorption occurs at lower temperature in the experiment, probably due to lateral interaction effects: model calculations were indeed performed in the zero-coverage limit, as already observed.

4. Conclusions

Ethanol decomposition on Pt(111) has been described using simple phenomenological model calculations and the results were compared to previous experimental and computational data.

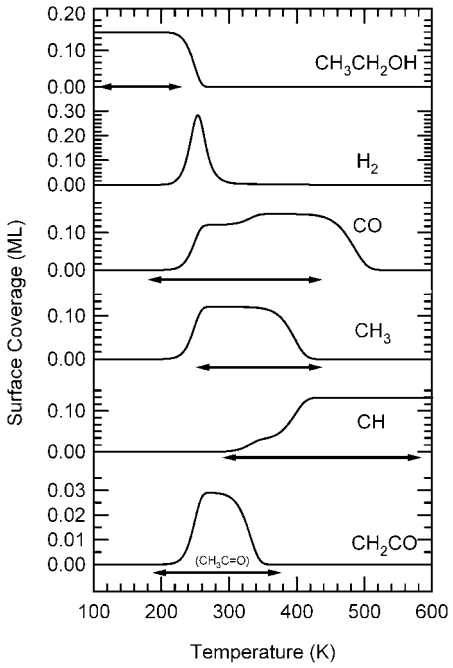

Figure 5. Surface concentration of the stable species during a simulated ethanol decomposition experiment on Pt(111), as a function of temperature (heating rate: 0.4 K s^{-1}), obtained on the basis of the results obtained with the simple UBI-QEP model. Arrows indicate the temperature range in which the species are found to be stable on the basis of real time temperature dependent XPS data [6].

It has been shown that quantitative agreement can also be obtained when calculating zero-coverage heats of adsorption and reaction barriers. A correlation between errors in the calculated binding energies and the bond lengths was found. It was also shown that care has to be taken in choosing the input values, depending on the source, due to differences in absolute values (within DFT frameworks) and discrepancies with experimental values. Calculated C–C and C–O decomposition barriers are not in line with data from DFT calculations, which appear to be too high, while reaction barriers for C–C scission obtained with the model are in line with the experiment. The model reproduces well the dehydrogenation barriers, as seen from the complete reaction simulation. Finally, the BEP linear relationship between transition and final state energies for the reactions considered is maintained.

The kinetic picture suggested by the UBI-QEP calculation for EtOH decomposition on Pt(111) is compatible with both previous DFT and experimental work and can explain their discrepancies. The proposed reaction mechanism predicts the formation of CH_3 and CH groups on the surface by distinct parallel reaction paths. In a second step, the methyl groups can rehydrogenate to methane, thus explaining the mass 14 peak observed in the TPD measurements, or dissociate to surface carbon and hydrogen. The proposed stable intermediate is CH_2CO, which is not in contrast with the spectroscopic data, where CH_3CO was only tentatively proposed.

Acknowledgments

We thank M Peressi and J A Dumesic for helpful discussions. We acknowledge financial support by MIUR under programmes COFIN2003 and FIRB2001.

References

[1] Deluga G A, Salge J R, Schmidt L D and Verykios X E 2004 *Science* **303** 993
[2] Cortright R D, Davda R R and Dumesic J A 2002 *Nature* **418** 964
[3] Alcala R, Mavrikakis M and Dumesic J A 2003 *J. Catal.* **218** 178
[4] Cases F, Morallon E, Vazquez J L, Perez K M and Aldaz A 1993 *J. Electroanal. Chem.* **350** 267
[5] Rajumon M K, Roberts R S, Wang F and Wells P B 1998 *J. Chem. Soc. Faraday Trans.* **94** 3699
[6] Lee A F, Gawthrope D E, Hart N J and Wilson K 2004 *Surf. Sci.* **548** 200
[7] Shustorovich E 1986 *Surf. Sci. Rep.* **6** 1
[8] Shustorovich E and Sellers H 1998 *Surf. Sci. Rep.* **31** 1
[9] Zeigarnik A, Valdes-Perez R and Egorova N 2001 *Surf. Sci.* **146** 158
[10] Blanskby S J and Ellison G B 2003 *Acc. Chem. Res.* **36** 255
[11] March J 1985 *Advanced Organic Chemistry: Reactions, Mechanisms and Structure* (New York: Wiley)
[12] Olivera P P, Patrito E M and Sellers H 1995 *Surf. Sci.* **327** 330
[13] Parker D, Bartram M and Koel B 1989 *Surf. Sci.* **217** 489
[14] Greeley J and Mavrikakis M 2004 *J. Am. Chem. Soc.* **126** 3910
[15] Greeley J and Mavrikakis M 2002 *J. Am. Chem. Soc.* **124** 7193
[16] Ishikawa Y, Liao M and Cabrera C 2004 *Theor. Comput. Chem.* **15** 325
[17] Kua J and Goddard W A 1998 *J. Phys. Chem.* B **102** 9492
[18] Liu Z and Hu P 2001 *J. Chem. Phys.* **114** 19
[19] Bransden B H and Joachain C J 1983 *Physics of Atoms and Molecules* (London: Longman)
[20] Bligaard T, Nørskov J K, Dahl S, Matthiensen J, Christensen C H and Sehested J 2004 *J. Catal.* **224** 206
[21] Nørskov J K, Bligaard T, Logadottir A, Bahn S, Hansen L B, Bollinger M, Bengaard H, Hammer B, Sljivancanin Z, Mavrikakis M, Xu Y, Dahl S and Jacobsen C J H 2002 *J. Catal.* **209** 275
[22] Fairbrother D H, Peng X D, Trenary M and Stairm P C 1995 *J. Chem. Soc. Faraday Trans.* **91** 3619
[23] Zaera F 1991 *Langmuir* **7** 1998
[24] Bunnik B S and Kramer G J 2003 *Methane Activation and the Rhodium Surface* Liverpool, UK (Conference Poster)